Environ Earth Sci (2016) 75:187
DOI 10.1007/s12665-015-5070-7

ORIGINAL ARTICLE

Hydrochemical assessment of surface water in watersheds near the Uranium Mining and Milling Facilities of Caldas, Brazil

C. A. de Carvalho Filho[1] · R. M. Moreira[2] · B. F. Guimarães[2] · V. V. M. Ferreira[2] · L. M. L. A. Auler[2] · H. E. L. Palmieri[2] · A. F. Oliveira[1] · P. H. Dutra[1]

Received: 5 February 2015 / Accepted: 7 September 2015

Abstract Sited in the Poços de Caldas Plateau, in southeastern Brazil, the Uranium Mining and Milling Facilities (UMMF) of Caldas are in the process of decommissioning. The main environmental problem in this site is the generation of acid mine drainage (AMD) in the tailings dam, open pit and waste rock piles. The aim of this work is to evaluate, by hydrochemical studies, the influence of acidic effluents from the Caldas UMMF, on the hydrochemistry of surface water along three watersheds: Consulta Brook, Soberbo Creek and Taquari River. Twelve sampling stations were established to carry out the investigation. Two of them were located at effluent retention ponds. Sampling was performed in the rainy and dry seasons of 2011, and the measured parameters were Eh, pH, EC (electrical conductivity), SO_4^{2-}, HCO_3^-, Cl^-, Na^+, K^+, Ca^{2+}, Mg^{2+} and Fe. The results have shown that iron is not a main constituent of the ionic composition of the local AMD. It could also be observed that acidic effluents were being discharged from retention ponds into the watercourses, causing a pronounced increase of the sulfate and calcium concentrations downstream. To trace the AMD migration the $(SO_4^{2-}/HCO_3^-)/(Na^+ + K^+/Ca^{2+})$ ratio was used. A detailed investigation of the near-surface groundwater is recommended downstream of the effluent ponds sites to evaluate the need for mitigating actions such as constructing hydraulic barriers. The present article shows that using simple techniques, such as Eh–pH and Piper diagrams, it is possible to depict the AMD fluvial migration pattern, which is an important information both to the authority responsible incumbent upon the remediation of the site, and to the affected interested parties who inhabit the impacted region.

Keywords Hydrochemistry · Acid mine drainage · Uranium mining · Major ions · Piper diagram

Introduction

One of the most relevant environmental impacts caused by mining industry activities is the generation of acidic discharges. This is normally referred to as acid mine drainage (AMD), the percolate that results from oxidation of sulfide minerals, when exposed to the combined action of water and oxygen. Bacteria of the genera *Thiobacillus* and *Leptospirillum* act as catalysts in this reaction. Pyrite (FeS_2) is the main mineral that undergoes this process. Mineral production activities are responsible for exposing large volumes of rocks and waste containing sulfide minerals. This significantly raises the oxidation and mobilization rates of metals by increasing the area that is exposed to air. As a consequence, acidic discharges produced by mining can threaten the quality of neighboring water resources. The main features of AMD are low pH (generally lower than 4), high Fe, SO_4^{2-} concentrations and varying concentrations of toxic metals (U. S. EnvironmentaL Protection Agency—USEPA 1994; Drever 1997, Williams 1975; Canovas et al. 2007).

✉ C. A. de Carvalho Filho
calbertocf@gmail.com; cacf@cdtn.br

[1] Postgraduate Program in Science and Technology Radiation, Minerals and Materials, Nuclear Technology Development Center (CDTN/CNEN), Av. Presidente Antônio Carlos, 6627, Pampulha, Belo Horizonte, MG 31270-901, Brazil

[2] Nuclear Technology Development Center (CDTN/CNEN), Av. Presidente Antônio Carlos, 6627, Pampulha, Belo Horizonte, MG 31270-901, Brazil

Published online: 25 January 2016

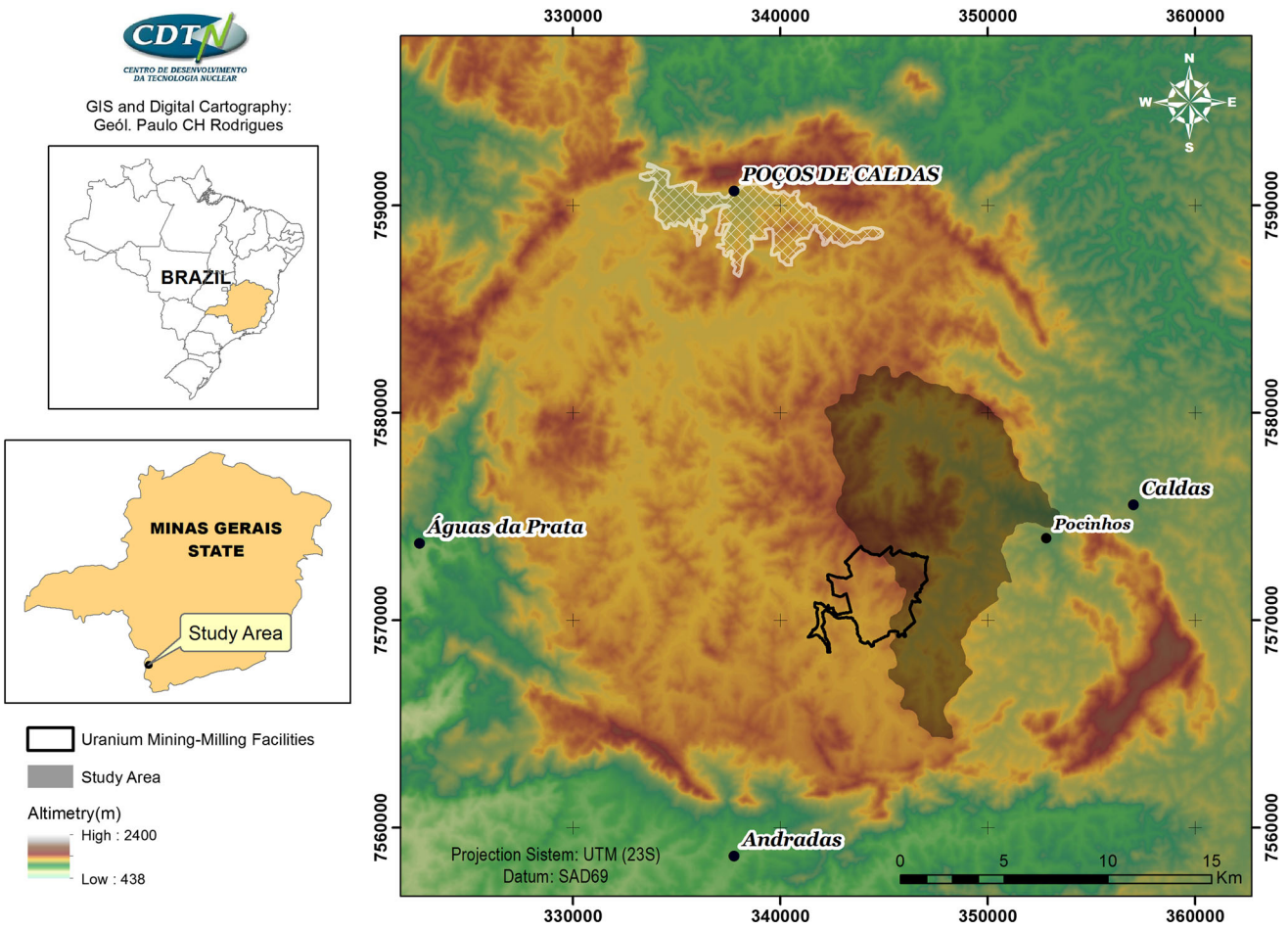

Fig. 1 Location of the study area

The present study was carried out in the Uranium Mining and Milling Facilities (UMMF) located in the municipality of Caldas (Minas Gerais, Brazil) which is controlled by the state owned company Nuclear Industries of Brazil (INB), presently undergoing a decommissioning process. The Caldas UMMF was the first facility to produce uranium in Brazil, starting its activities in 1982 and being definitely closed in 1995. During these 13 years of operation, 1242 ton of yellowcake were produced, generating 44.8 $\times$ 10^6 m^3 of mining waste and 2.39 $\times$ 10^6 m^3 of waste from chemical process or tailings waste (Majdalani and Tavares 2001). AMD is considered the main environmental impact in the UMMF of Caldas, and resulted from the oxidation of sulfide minerals, mainly pyrite, in uranium ore and host rocks. It was generated in the mine pit, in the milling wastes that were deposited in the tailings dam (TD), and in the two main waste rock piles (WRP): WRP4 and WRP8 (Fernandes et al. 1995, 1996, 1998, 2008; Fernandes and Franklin 2001; Cipriani 2002; Franklin 2007; Campos et al. 2011, Rodgher et al. 2013). The present work is part of a set of research activities being coordinated by the National Institute of Science and Technology on Mineral Resources, Water, and Biodiversity—INCT-Acqua. The Institute aims to assess sites contaminated by mining activities and develop and implement remediation techniques, thus providing accurate information that leads to a better governance of the mining territories and to a more thorough understanding of environmental issues by the stakeholders. The objective of this article is to investigate, mainly by the analysis of major ions, whether the acidic effluent generated by Caldas UMMF is altering the hydrochemistry of the local surface waters.

Study area and waste deposits

The Caldas UMMF is located in the Poços de Caldas Plateau, in the southeastern part of Brazil (Fig. 1), within a circular alkaline (30–35 km in diameter) volcanic caldera. The local geology comprises a suite of alkaline volcanic and plutonic rocks belonging to the Poços de Caldas

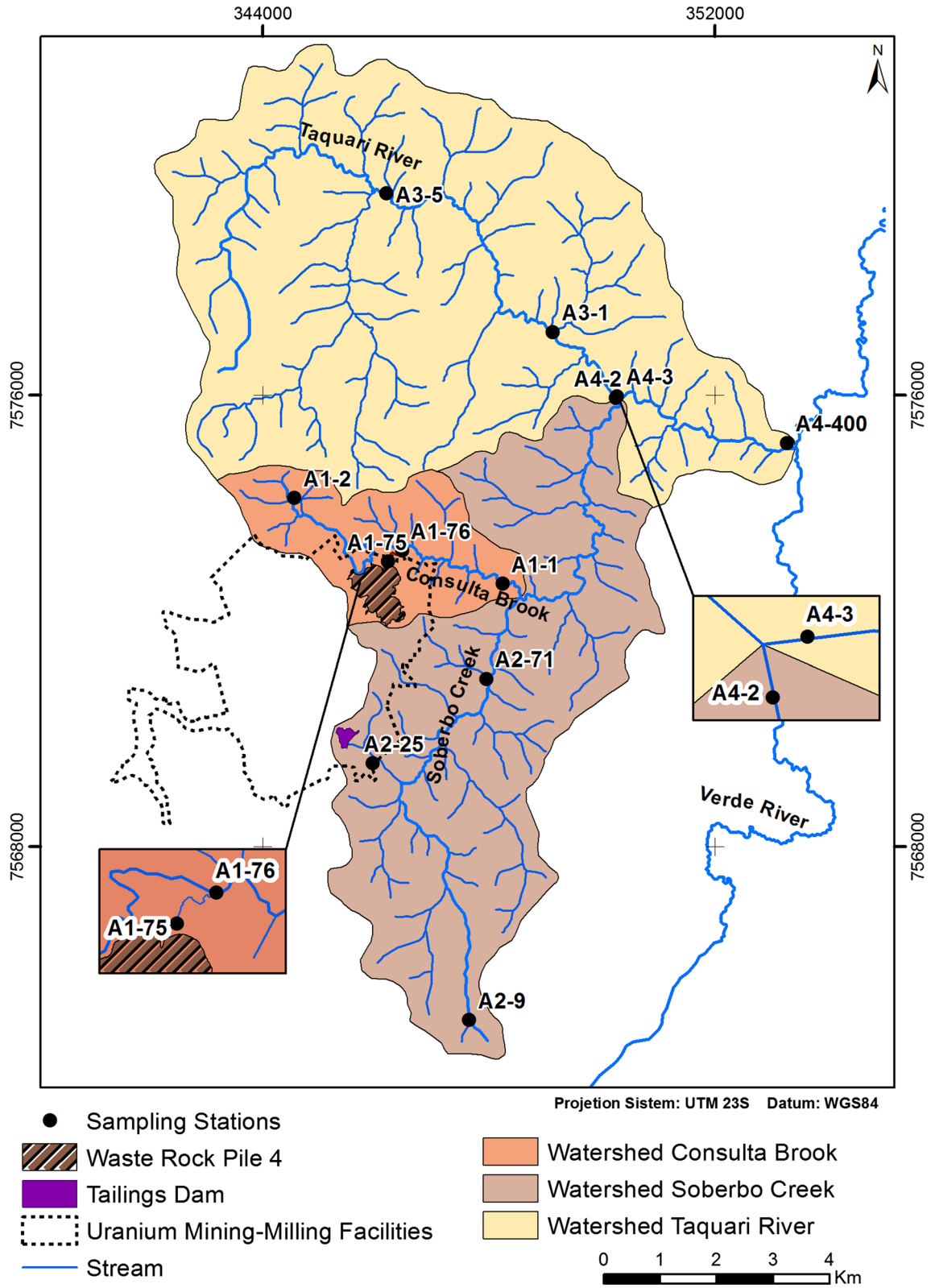

Fig. 2 Map of the study area and distribution of the sampling stations

alkaline complex that represents the largest known alkaline complex in South America and one of the largest in the world (Woolley 1987).

The lithology of the uranium deposit is composed of volcanic and subvolcanic phonolites, nepheline syenites and volcanic breccia pipes. Various alkaline rocks on the site have been affected by a large hydrothermal event (solutions enriched in K-S), which led to pyritization, potassium metasomatism and primary mineralization of uranium. Intense weathering, associated with downward migrating oxidizing groundwater, has resulted in a secondary supergene enrichment of uranium along redox fronts. The ore is mainly made up of uranium oxides (uraninite and pitchblende), sulfide minerals (mainly pyrite), zirconium minerals, fluorite, REE phases and Mo-bearing minerals (Schorscher and Shea 1992; Waber et al. 1992). The water divide of two watersheds, Antas and Verde rivers, crosses the Caldas UMMF. Waters from these watersheds are used for cattle watering and for crop irrigation (mostly silviculture).

The study area is about 100 km^2, partially compassing the Caldas UMMF premises and encompassing three small watersheds: the Taquari River (Verde River tributary), the Soberbo Creek and the Consulta Brook (Fig. 2). The annual average temperature is 19 °C, varying between 1 and 36 °C. The average annual rainfall in the region is around 1700 mm, with 80 % of the rain concentrated between October and March (Franklin 2007). The uranium ore was mined in an open pit, covering an area of about 15 km^2. It was estimated that 94.5×10^6 ton of rock was removed, but only 2 % of this amount was sent to physical and chemical processing. The remainder has been stored in two main waste rock piles (WRP): named Number 4 (WRP4) and Number 8 (WRP8), of which only the first one is inside the study area, in the Consulta Brook watershed. Briefly, the milling process consisted in the addition of an oxidant (pyrolusite) to the ore and subsequent sulfuric acid leaching. Following this, uranium was extracted from the liquid solution with an organic solvent and precipitated with NH_4OH. This chemical processing produced large quantities of liquid and solid wastes, which, after neutralization by $CaCO_3$ and CaO addition, were released into and pumped to the TD (sited in Soberbo watershed) for solid deposition (Fig. 2) (Fernandes et al. 1995, 1996).

The WRP4 pile has been erected right upon the former course of the Consulta Brook (Fig. 2), which thenceforth had to be diverted through a channel. The WRP4 has an area of 56.4 ha and contains 14.26 million m^3 of waste rocks. The maximum height of the pile is 90 m and its slope reaches up to 70°. The exposure of a large volume of pyritic waste leads to AMD being generated inside the pile. Most of the acidic water that percolates throughout the WRP4 is collected in an effluent retention pond (BNF) located at the base of the WRP4 pile. The liquid effluent from the WRP4 normally has a pH value between 3 and 4 and high concentrations of U, Al, Mn, F and SO_4^{2-} (Fernandes et al. 1995; Franklin 2007). This effluent retained at BNF is pumped to an acid water treatment unit where it is neutralized with calcium hydroxide $Ca(OH)_2$, generating a high-pH (pH 10–12) sludge that until 1998 was pumped to the TD, and since then is being discharged in the open pit, following the exhaustion of the dam capacity to receive additional wastes. This sludge presents contaminants such as U, Mn, F, Zn and Fe, and a high concentration of Al^{3+}, Ca^{2+}, OH^- and SO_4^{2-} ions (Gomes et al. 2012). The neutralized overflow is released into the Antas River, which is not part of this study.

The TD was built in the talweg of a small Soberbo Creek affluent (Fig. 2). Its flooded area comprises about 0.23–0.25 km^2 and its drainage area is 0.86 km^2. Around 4×10^6 t of radioactive waste is deposited in the TD, mainly, waste generated from ore processing (Golder Associates Brazil Consulting and Projects Ltd 2012). Outstanding constituents of the solid material in the TD are Ca, U, Th, Mn, ^{226}Ra, ^{210}Pb and SO_4^{2-} (Fernandes et al. 1996; Golder Associates Brazil Consulting and Projects Ltd 2012). During the milling processes, pyrite was only partially oxidized, its oxidation being complete in the TD, hence contributing to the AMD generation in this dam (Cipriani 2002; Fernandes et al. 1995). The liquid effluent from the TD is treated with barium chloride ($BaCl_2$) to precipitate radium in the form of sulfate $(Ba,Ra)SO_4$. The precipitate is retained in two settling ponds (D1 and D2) and the liquid effluent that passes through D2 is released to the environment, i.e. the downstream course of the Soberbo Creek.

Table 1 Electrical conductivity (EC) and corresponding maximum allowable ionic balance error (MAE)

EC (μS/cm)	50	200	500	2000	>2000
MAE (%)	30	10	8	4	<4

Methodology

A total of 12 sampling stations have been established (Fig. 2). Two of them were located within the effluent ponds; station A1-75 at BNF and station A2-25 at D2. Four stations were positioned upstream of the Caldas UMMF; A1-2 at the Consulta Brook, A2-9 at the Soberbo Creek, and both A3-1 and A3-5 at the Taquari River. The remaining stations were located downstream of the Caldas UMMF. In total, 24 surface water samples were collected during the dry and wet seasons in 2011, i.e. two samples

Table 2 Results from the ionic analysis (meq/L), sum of cations (c) and anions (Σa) concentrations, pH, Eh, electrical conductivity (EC, μS/cm,), ionic balance error $E_p(\%)$ and total iron (Fetot, mg/L)

Station	Na^+	K^+	Ca^{2+}	Mg^{2+}	Σc	SO_4^{2-}	Cl^-	HCO_3^-	Σa	Eh(v)	EC	pH	E_p	Fetot
Rainy season														
A1-2	0.008	0.076	0.032	0.011	0.128	0.006	0.006	0.131	0.143	0.372	18.90	5.98	11.16	1.40
A1-75	0.209	0.292	4.790	0.749	6.039	22.940	0.140	IN	23.080	0.582	1766.0	3.82	***117.04***	0.84
A1-76	0.018	0.096	0.240	0.053	0.406	1.118	0.006	0.066	1.190	0.502	130.70	4.52	***98.21***	0.75
A1-1	0.017	0.094	0.125	0.028	0.264	0.437	0.007	0.066	0.510	0.449	60.95	5.01	***63.69***	0.54
A2-9	0.060	0.060	0.080	0.038	0.238	0.007	0.006	0.262	0.275	0.327	28.02	6.26	14.53	0.40
A2-25	0.100	0.206	7.435	0.063	7.805	7.624	0.077	0.344	8.046	0.511	765.30	6.08	3.04	0.56
A2-71	0.050	0.086	0.314	0.021	0.472	0.260	0.006	0.197	0.463	0.391	53.44	6.61	1.91	0.26
A4-2	0.043	0.085	0.175	0.018	0.321	0.206	0.007	0.148	0.361	0.371	43.72	6.50	11.71	0.22
A3-5	0.048	0.088	0.055	0.013	0.204	0.005	0.007	0.213	0.225	0.450	17.92	6.02	9.83	0.74
A3-1	0.047	0.086	0.041	0.011	0.185	0.006	0.007	0.213	0.226	0.500	17.39	6.40	20.07	1.10
A4-3	0.043	0.082	0.100	0.020	0.245	0.098	0.007	0.148	0.253	0.455	29.08	6.50	3.39	0.35
A4-400	0.050	0.083	0.100	0.016	0.248	0.099	0.007	0.164	0.270	0.344	28.68	6.50	8.21	0.32
Dry season														
A1-2	0.007	0.070	0.022	0.008	0.106	0.006	0.006	0.100	0.112	0.401	11.14	6.15	4.96	0.92
A1-75	0.055	0.228	3.892	0.625	4.801	20.964	0.006	IN	20.970	0.558	1629.0	3.65	***125.48***	0.84
A1-76	0.015	0.093	0.424	0.082	0.614	1.853	0.008	0.051	1.911	0.488	185.60	4.64	***102.71***	0.86
A1-1	0.018	0.083	0.180	0.038	0.318	0.470	0.006	0.051	0.527	0.506	107.50	4.64	***49.35***	0.37
A2-9	0.083	0.069	0.105	0.073	0.330	0.006	0.009	0.213	0.229	0.276	42.24	6.19	36.3	0.92
A2-25	0.187	0.206	8.034	0.099	8.526	9.243	0.096	0.344	9.683	0.496	850.20	6.18	***12.72***	0.10
A2-71	0.056	0.077	0.429	0.028	0.590	0.416	0.012	0.180	0.609	0.488	67.38	6.15	3.14	0.11
A4-2	0.043	0.073	0.190	0.021	0.325	0.291	0.006	0.116	0.413	0.459	46.99	6.10	23.83	0.10
A3-5	0.048	0.069	0.042	0.010	0.169	0.008	0.006	0.164	0.178	0.372	19.20	5.90	5.52	0.34
A3-1	0.051	0.072	0.046	0.011	0.180	0.008	0.007	0.164	0.179	0.495	22.64	5.95	0.80	0.27
A4-3	0.045	0.070	0.110	0.015	0.239	0.139	0.007	0.164	0.310	0.465	34.01	6.02	25.82	0.17
A4-400	0.050	0.071	0.105	0.015	0.240	0.125	0.007	0.151	0.283	0.455	31.70	5.90	16.17	0.16

IN inexistent; E_p values in italics boldface are not in accordance with the maximum allowable ionic balance error (MAE)

per station. The parameters pH, Eh (redox potential) and electrical conductivity (EC) were measured in situ, using an Ultrameter II multi-parameter handheld meter (Myron L Company). The water samples were collected in properly cleaned polyethylene flasks (500 mL). Each flask was thoroughly rinsed with sample water prior to sampling itself. After the collection, the samples were filtered through 0.45 μm membrane filters; samples for cation determination being acidified with HNO_3 (pH $\sim$ 2). The flasks were duly packed in thermally insulated cases (±4 °C) and dispatched to the laboratory as soon as possible. The whole analytical work was carried out at the Nuclear Technology Development Center (CDTN/CNEN). Calcium, iron and magnesium were determined by inductively coupled plasma optical emission spectrometry (ICP-OES); sodium, potassium, chloride and sulfate ions were determined by ionic chromatography; bicarbonate and carbonate ions were titrated with standardized solutions. The analytical accuracy and precision were checked using reference materials and performing replicates.

The ionic error balance was the basis for evaluating the internal consistency of the analytical results. The value of this balance has been calculated for each sample according to Eq. 1 (Custódio 1983).

$$E_p = \left[\frac{\Sigma c - \Sigma a}{1/2(\Sigma c + \Sigma a)}\right] \times 100\% \quad (1)$$

where E_p ionic balance error (%), Σc total cationic concentration (meq/L), Σa total anionic concentration (meq/L). The maximum allowable ionic balance error (MAE) has been estimated as a function of the electrical conductance (EC) according to Table 1.

The measured ion concentrations were plotted in Piper and Stiff diagrams. Piper diagrams are commonly used in identifying similarities and differences in water compositions and typifying them (Chadha 1999). The Stiff diagrams are useful in making a rapid visual comparison between waters from different sources (Fetter 1994).The ionic concentration of each water sample was plotted in the Stiff diagrams and depicted in maps. The percent

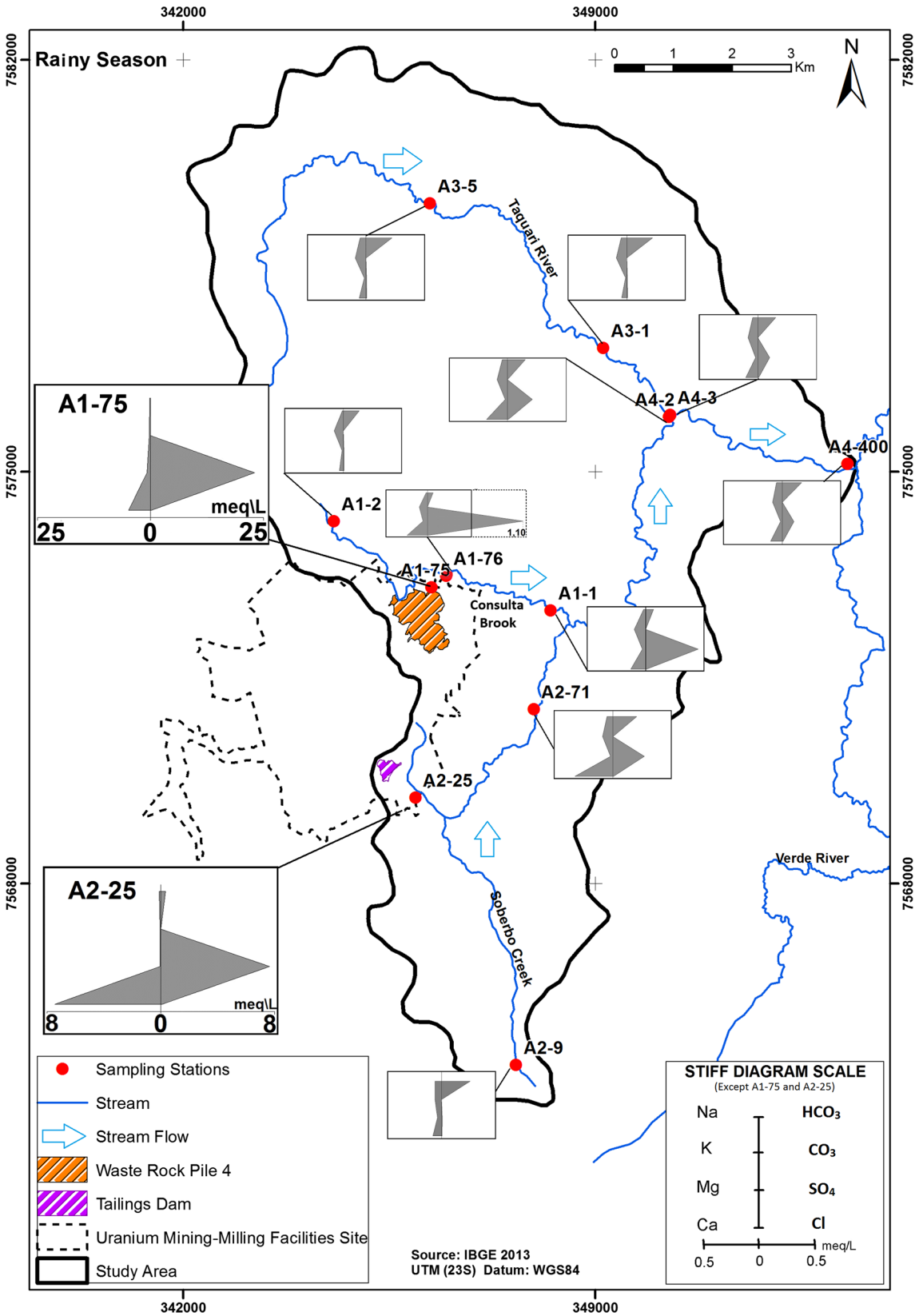

Fig. 3 Stiff diagrams for the rainy season

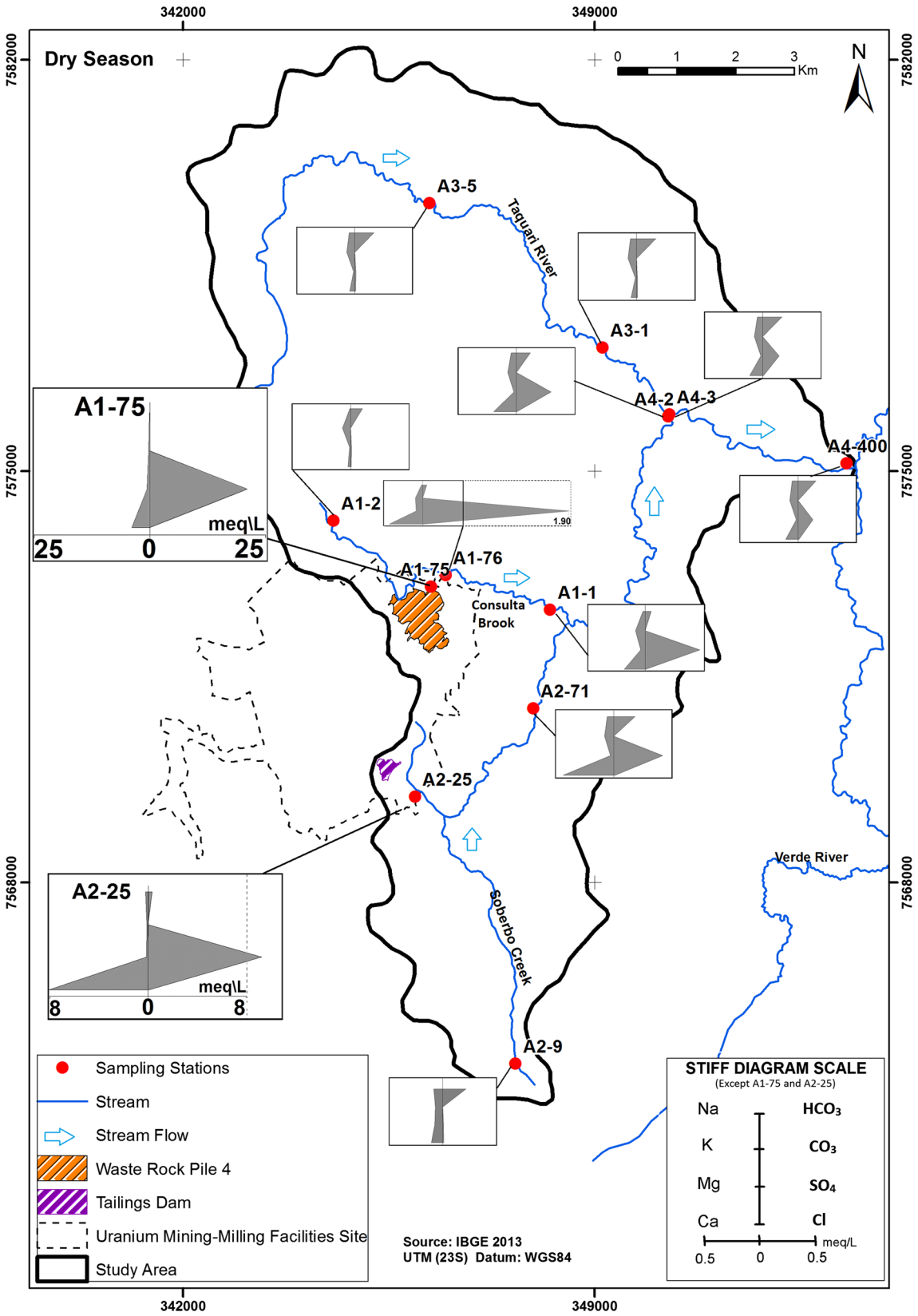

Fig. 4 Stiff diagrams for the dry season

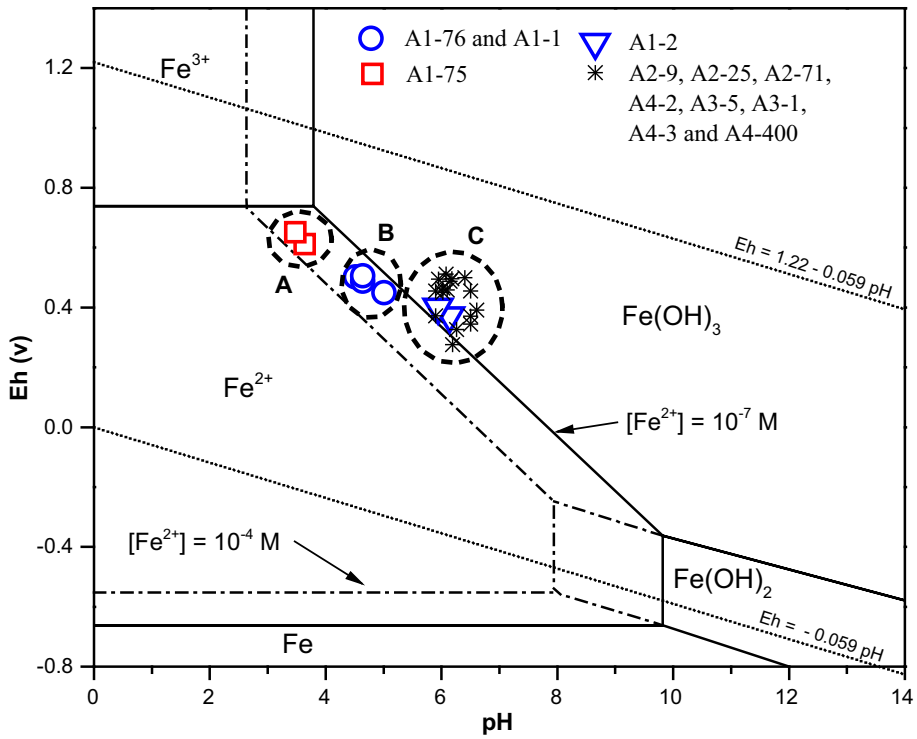

Fig. 5 Eh and pH measurements plotted on a Pourbaix diagram for the iron–water system (Garrals and Christ 1965)

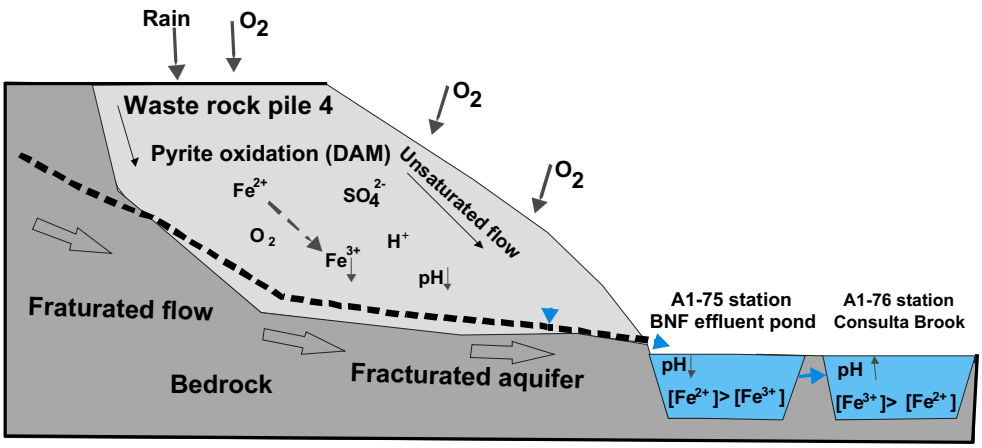

Fig. 6 Schematic representation of AMD generation as water flows inside the WRP4/BNF system

abundance of each cation and anion has been represented in a Piper diagram. The data were plotted on an Eh–pH diagram for the iron-water system to assess the iron oxidation state in the various samples, as well as their stability under the corresponding Eh–pH conditions.

Results and discussion

The values of ionic concentration, pH, EC and E_p determined for each water sample are presented in Table 2. The CO_3^{2-} species was inexistent in all samples, as well as HCO_3^- at station A1-75. The E_p values which are not in accordance with the MAE—EC correspondence (Table 1) are printed in italics boldface. As regards the Soberbo Creek, the calculated E_p value superseded the MAE only at station A2-25 (dry season). But in the Consulta Brook the MAE was superseded, at stations A1-75, A1-76 and A1-1 in both seasons. All the samples from Taquari River displayed E_p values lower than the MAE. This noncompliance with the MAE is seemingly related to AMD causing high concentrations of ionic species in water, besides the contribution of dissolved species other than the major ions. It can be observed that those samples in which E_p > MAE

Table 3 Relative abundance (%) of cations and anions

Station	$Na^+ + K^+$	Ca^{2+}	Mg^{2+}	SO_4^{2-}	Cl^-	$CO_3^{2-} + HCO_3^-$
Rainy season						
A1-2	66	25	8	4	4	92
A1-75	8	79	12	99	1	0
A1-76	28	59	13	94	1	6
A1-1	42	47	11	86	1	13
A2-9	50	34	16	2	2	95
A2-25	4	95	1	95	1	4
A2-71	29	67	5	56	1	43
A4-2	40	54	6	57	2	41
A3-5	67	27	6	2	3	95
A3-1	72	22	6	2	3	94
A4-3	51	41	8	39	3	58
A4-400	54	40	6	37	3	61
Dry season						
A1-2	72	21	8	5	5	90
A1-75	6	81	13	100	0	0
A1-76	18	69	13	97	0	3
A1-1	32	56	12	89	1	10
A2-9	46	32	22	3	4	93
A2-25	5	94	1	95	1	4
A2-71	23	73	5	68	2	30
A4-2	35	58	6	70	1	28
A3-5	69	25	6	5	3	92
A3-1	68	26	6	4	4	92
A4-3	48	46	6	45	2	53
A4-400	50	44	6	44	2	53

(with exception of the sample at A2-25 station) display EC values above 60 μS/cm and pH $\leq$ 5. The calculated E_p values for the samples from stations A1-76 and A1-1 in the Consulta Brook are indicative of acid effluent discharges from station A1-75 to Consulta brook.

Examining Fig. 3 and Fig. 4, prepared with the data from Table 2, it can be noticed that the Stiff diagrams relative to the two water sampling campaigns are quite similar. The sampling stations at the effluent discharge positions (A1-75 and A2-25) show higher concentrations of Ca^{2+} and SO_4^{2-}. The water samples downstream of the effluent discharge points are enriched in Ca^{2+} and SO_4^{2-} in comparison with the stations upstream. This is an indication of the impact of the effluents from the Caldas UMMF on the surface waters downstream of the discharge sections.

Looking at the Pourbaix diagram drawn in Fig. 5, one can discern three distinct groups constituted by the samples from stations A1-75 (A), A1-76 and A1-1 (B) and A1-2 and the remaining stations (C). Considering only the Consulta Brook, it is possible to conclude that water coming from station A1-2 and that receive the discharge from the effluent station A1-75 have become more acidic and oxidizing when it reaches stations A1-76 and A1-1. Regarding iron, Fig. 5 confirms that water at stations A1-76 and A1-1 are a mixture of the effluents from station A1-75, that are richer in Fe(II), with the upstream waters of the Consulta Brook (A1-2 station) which is richer in Fe(III). This has also been noticed by Campos et al. (2011) who found the Fe(II) concentration at station A1-75 was twice as high as that of Fe(III), whereas the Fe(III) concentration at A1-76 was four times higher than that of Fe(II).

The changes in the system Eh–pH values (Fig. 5) causing a shift in the iron oxidation state within the WRP4/BNF effluent pond system (into which is sited A1-75 station) and later on at the Consulta Brook can be explained by the pyrite oxidation process referring to Fig. 6 and the set of chemical reactions (Eqs. 2, 3 and 4) (Williamson and Rimstidt 1994; Ptacek and Blowes 2003). As shown in Fig. 6 the WRP4 waste pile is located in between a water recharge and a water discharge region. Recharge proceeds from rain water infiltration, but also from seepage through the laterals of the Consulta Brook

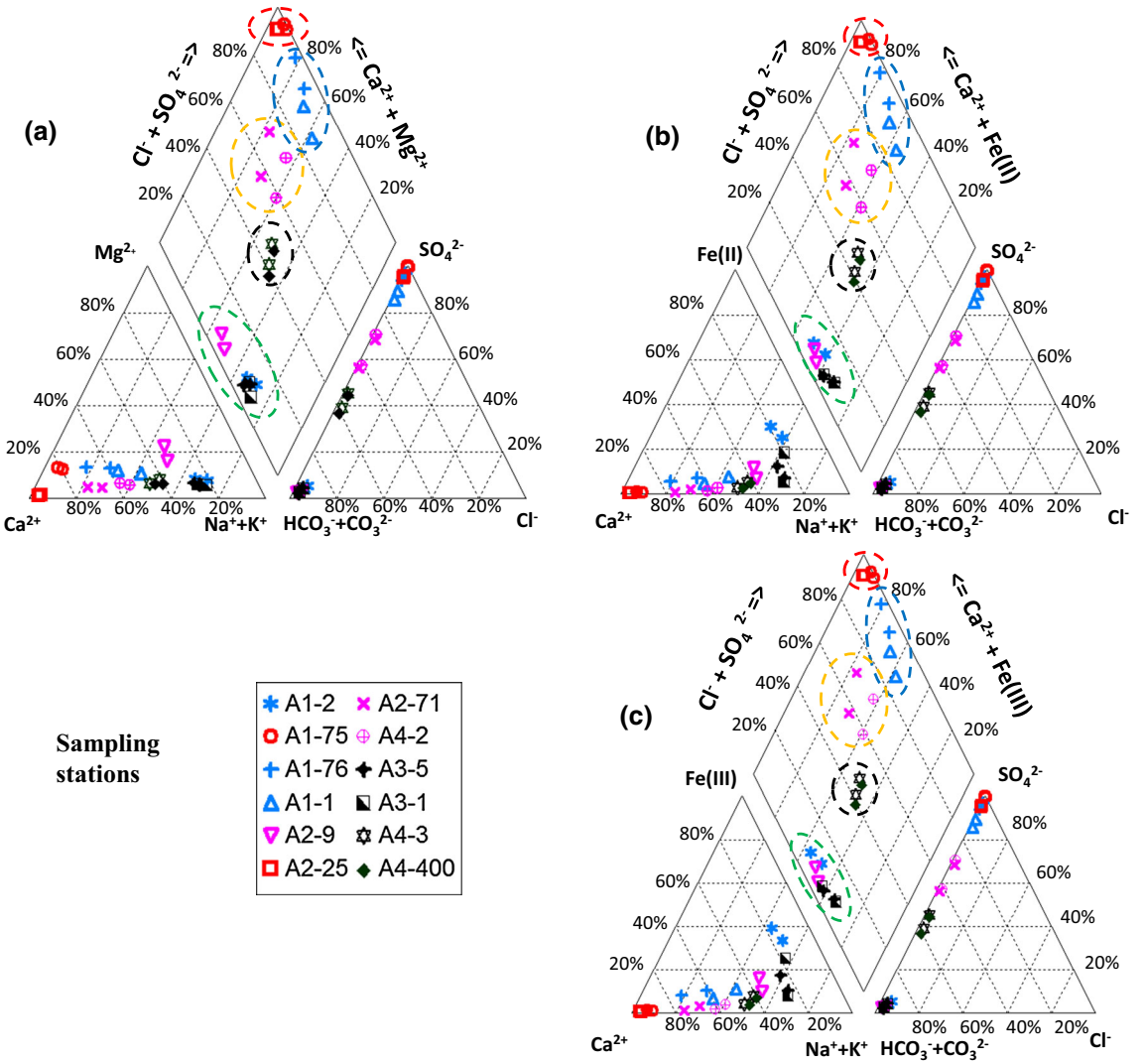

Fig. 7 Piper diagrams of all collected samples. **a** with Mg^{2+}; **b** and **c** with Fe(II) and Fe(III) replacing Mg^{2+}, respectively. The samples from Consulta Brook are in *blue*, those from Soberbo Creek in *pink*, those from Taquari River in *black*, and those from the effluent ponds in *red*. The *green dashed circle* surrounding the stations located upstream of the Caldas UMMF, while the *red circles* comprise effluents ponds. The *other circles* represent the stations downstream of the UMMF: *blue* (Consulta Brook); *brown* (Soberbo Creek); and *black* (Taquari River)

diversion channel (Franklin 2007). The water discharge is at the foot of the WRP4 pile, and puddles are formed at the place. The water flows inside WRP4 in a predominantly non-saturated environment, since the grain size distribution and heterogeneity in the pile favor oxygenation and the inception of the AMD process. Hence, pyrite oxidation leads to the release of large amounts of SO_4^{2-}, H^+ and Fe(II) (Eq. 2). The released Fe(II) can be further oxidized to Fe(III) (Eq. 3), and as such can oxidize more pyrite, once again generating Fe(II), together with SO_4^{2-} and H^+ (Eq. 4). Depending on the amount of Fe(II) oxidation a variety of Fe-bearing secondary solids can form, for instance, Fe(II)-sulfate salts, and Fe(III) oxide-hydroxides (Jambor 2003).

$$FeS_{2(s)} + \frac{7}{2}O_{2(g)} + H_2O_{(l)} \rightarrow Fe^{2+}_{(aq)} + 2SO^{2-}_{4(aq)} + 2H^{+}_{(aq)} \quad (2)$$

$$Fe^{2+}_{(aq)} + \frac{1}{4}O_{2(g)} + \frac{5}{2}H_2O \rightarrow Fe(OH)_{3(s)} + 2H^{+}_{(aq)} \quad (3)$$

$$FeS_{2(s)} + 14Fe^{3+}_{(aq)} + 8H_2O_{(l)} \rightarrow 15Fe^{2+}_{(aq)} + 2\,SO^{2-}_{4(aq)} + 16H^{+}_{(aq)} \quad (4)$$

As water penetrates towards the saturated zone (Fig. 6), the environment becomes more anoxic and the oxidation processes slow down, the reduced iron species predominate. But as soon as the water is discharged at station A1-75 the pH is raised and Fe(II) oxidation is increased anew.

Table 4 Relative abundance (%) of cations

Station	% Cations			% Cations		
	$Na^+ + K^+$	Ca^{2+}	Fe^{2+}	$Na^+ + K^+$	Ca^{2+}	Fe^{3+}
Rainy season						
A1-2	51	19	30	44	17	39
A1-75	9	90	1	9	90	1
A1-76	30	63	7	29	61	10
A1-1	43	49	8	42	47	11
A2-9	56	37	7	54	36	10
A2-25	4	96	0	4	96	0
A2-71	30	68	2	29	68	3
A4-2	41	56	3	41	56	4
A3-5	63	25	12	59	24	17
A3-1	62	19	18	57	18	25
A4-3	53	42	5	51	41	8
A4-400	54	41	5	53	40	7
Dry season						
A1-2	58	17	25	52	15	34
A1-75	7	93	1	7	92	1
A1-76	19	75	5	19	73	8
A1-1	34	61	5	34	60	7
A2-9	52	36	11	50	34	16
A2-25	5	95	0	5	95	0
A2-71	24	76	1	23	76	1
A4-2	37	61	1	37	61	2
A3-5	68	25	7	66	24	10
A3-1	69	26	5	67	25	8
A4-3	50	48	3	49	47	4
A4-400	52	45	2	52	45	4

This can be visually checked on site by the characteristic brownish-yellowish-reddish sludge, known as yellow boy, that dye the banks at this place. The behavior of iron in the water percolating through the WRP4 has also been described by Franklin (2007) when analyzing the chemical composition of this water. She concluded that there is an accumulation of secondary iron minerals relatively to the sulfate minerals, pointing to a higher mobilization of S and precipitation of Fe. This control exerted by oxygen concentration and pH over iron oxidation inside the WRP4 is similar to that described by Fernandes et al. (1996) in the context of the tailings dam (TD).

The results in Table 3 were plotted on a Piper diagram (Fig. 7a), which shows that Ca^{2+}, $Na^+ + K^+$, SO_4^{2-} and HCO_3^- are the more significant ions from the hydrochemical viewpoint. The effluents at station A1-75 are characterized by a higher abundance in Ca^{2+} and SO_4^{2-}. On the other hand, the waters at station A1-2, which is upstream of the discharge (A1-75 station), distinguishes itself by its predominance in $Na^+ + K^+$ and HCO_3^-, whereas Ca^{2+} and SO_4^{2-} are less abundant. Enrichment in Ca^{2+} and SO_4^{2-} can be noticed at stations A1-76 and A1-1 as compared to station A1-2, which suggests that they are being impacted by the effluents discharged at station A1-75.

Looking at the Soberbo Creek watershed, it can be seen that the effluent from station A2-25 contains more Ca^{2+} and SO_4^{2-} (Fig. 7a). The water in station A2-9, which is upstream of the discharge, are characterized by a larger abundance in $Na^+ + K^+$ and HCO_3^- and a lesser abundance in Ca^{2+} and SO_4^{2-}. It can be seen that downstream of the effluent discharge at station A2-25, there is an increase in the concentration of Ca^{2+} and SO_4^{2-} at station A2-71 and A4-2, when compared to station A2-9. This is an indication that effluent from station A2-25 caused an increase in the ionic concentration in the Soberbo Creek downstream its discharge point. The water at stations A3-5 and A3-1 in Taquari River, located upstream of the confluence with the Soberbo Creek, exhibit a predominance of $Na^+ + K^+$ and HCO_3^-, and a lesser abundance of Ca^{2+} and SO_4^{2-}. The water at stations A4-3 and A4-400, downstream of the Soberbo Creek discharge, are enriched with Ca^{2+} and in SO_4^{2-} in comparison to the upstream stations, showing that the impact of the Caldas UMMF and extends all the way into the Taquari River.

It is noted that in the stations situated downstream of the Caldas UMMF, there is a higher ionic similarity of its waters with that of the effluents the closer they are to the A1-75 and A2-25 discharge stations, in other words, they are more enriched in Ca^{2+} and SO_4^{2-}. On the other hand, the farther these stations are from the effluent discharge sites, the more similar their water ionic composition is to those upstream of the Caldas UMMF. Consequently, they become less enriched in Ca^{2+} and SO_4^{2-} and more enriched in $Na^+ + K^+$ and in HCO_3^-, as shown in the dashed circles in Fig. 7a. The waters at stations sited upstream of the Caldas UMMF (A1-2, A2-9, A3-5 and A3-1) are typified as sodium–potassium bicarbonate and should depict the natural or geogenic ionic composition of the respective water streams. The effluents discharged at stations A1-75 and A2-25 show an ionic composition corresponding to the calcium-sulfate water type. It can be seen in Fig. 7a that the natural sodium-bicarbonate waters, upstream of the Caldas UMMF, are converted into the calcium-sulfate type immediately downstream of the effluent discharge stations, and thereafter progressively restored to their former condition as they move away, hinting at a natural recovery process.

The data in Table 4 were used in constructing Piper diagrams including iron in place of Mg^{2+}. Inasmuch as the total iron has been measured in the collected samples, in the soluble form, two diagrams have been composed; in

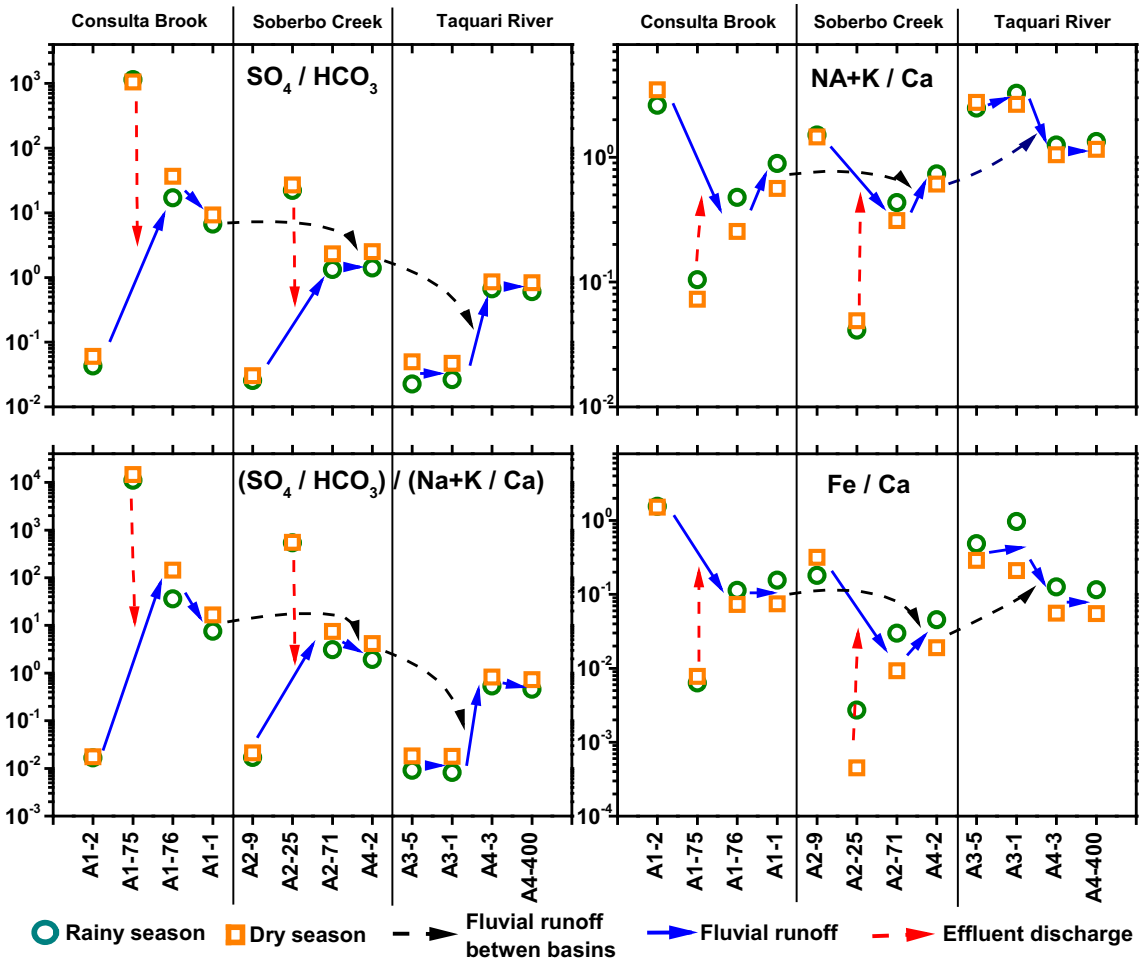

Fig. 8 Ionic ratios

one of them it has been assumed the totality of iron to be present as Fe(II) (Fig. 7b), whereas in the other diagram all the iron was assumed to be Fe(III) (Fig. 7c). Both diagrams are quite similar, and also the classification of the waters at the various sampling stations does not diverge from that shown at Fig. 7a, indicating that iron does not significantly participate in ionic equilibrium at the studied watershed. Only the water samples from stations A1-2 and A3-1 exhibit a somewhat higher enrichment in iron.

A comparison of the ionic ratios measured in all sampling stations of the study area is shown in Fig. 8. An HCO_3^- concentration of 1 mg/L (~0.02 meq/L) was adopted for station A1-75 to avoid dividing by zero (Table 2). All the graphs in Fig. 8 evince the influence of the effluents from stations A1-75 and A2-25. The water samples present higher SO_4^{2-} and Ca^{2+} concentrations downstream of the effluent discharge stations. This includes the water flowing from Consulta Brook to Soberbo Creek and from there to Taquari River. The SO_4^{2-}/HCO_3^- ratio was higher in the dry than in the rainy season, whereas the $Na^+ + K^+/Ca^{2+}$ ratio was lower, which is an indication of a more significant influence of the effluents in the dry season. Such a characteristic is better discerned by examining the trend of the $(SO4^{2-}/HCO_3^-)/(Na^+ + K^+/Ca^{2+})$ ratio. Comparing these ratios in the Piper diagrams, it is clear that the water quality downstream of the Caldas UMMF progressively drifts back towards the ionic ratios of the waters upstream of the mine.

Waters at stations A1-75 and A2-25, i.e. just prior to the discharge in the watershed system, the Fe/Ca ratio shows that iron is relatively less abundant than in all the stations in the watershed properly. As mentioned above, this may be due to the precipitation, mainly of the Fe(III) species inside the BNF effluent pond and the TD dam, respectively.

Relatively high SO_4^{2-} concentrations were observed at A1-75 and A2-25. This is unequivocally the result of the pyrite oxidation process and AMD generation (Eqs. 2, 3, 4) at WRP4 and TD, whose effluents directly flow past these stations. The relative abundance of Ca^{2+} in the effluent at station A1-75 and at station A2-25 is mainly due to the

combined effects of fluorite (CaF_2) dissolution inside WRP4 and TD (Eq. 5), and of the AMD action. The Ca^{2+} and SO_4^{2-} concentration at station A2-25 has also had a contribution from the calcium-based additives presently $Ca(OH)_2$ added to neutralize the acid effluents (Eqs. 6, 7, 8).

$$CaF_2(s) \rightarrow Ca^{2+}(aq) + 2F^{-}(aq) \quad (5)$$

$$H_2SO_4 + CaCO_3 \rightarrow Ca^{2+} + SO_4^{2-} + CO_2 + H_2O \quad (6)$$

$$H_2SO_4 + Ca(OH)_2 \rightarrow Ca^{2+} + SO_4^{2-} + 2H_2O \quad (7)$$

$$H_2SO_4 + CaO \rightarrow Ca^{2+} + SO_4^{2-} + H_2O \quad (8)$$

Conclusion

Comparative analysis of ionic composition using Piper and Stiff diagrams, as well as Eh–pH Pourbaix diagrams proved to be simple and efficient in evaluating the environmental impact of acidic effluents (AMD) from the Caldas UMMF on the nearby watershed downstream. It was also shown that although iron has an important role in the oxidation process and in the generation of acid drainage, it does not have a prominent participation in the ionic composition of the acid effluents in A1-75 station. On the other hand, SO_4^{2-} and Ca^{2+} are relevant constituents in the ionic composition of the effluents and their ionic ratios can be used for tracing effluent migration. In the studied case, the $(SO_4^{2-}/HCO_3^{-})/(Na^{+} + K^{+}/Ca^{2+})$ ratio is especially useful for this purpose. The paths, the patterns and the reach impacted by the effluents from the Caldas UMMF have also been defined using these tools. Further studies focusing the groundwater should be carried out to evaluate the need of enforcing mitigation actions such as erecting water barriers downstream of the discharges. Presently, some of these interventions are already being enforced by the Caldas UMMF operator.

Acknowledgments The authors are indebted to the Brazilian Scientific and Technological Development Council (CNPq), the Minas Gerais Foundation for Research Support (Fapemig) for financial support, the Brazilian Institute for Mineral, Water, and Biodiversity Resources (INCT-Acqua), and the Brazilian Nuclear Industries (INB) for operational and technical support.

References

Campos MB, Azevedo H, Nascimento MRL, Roque CV, Rodgher S (2011) Environmental assessment of water from a uranium mine (Caldas, Minas Gerais State, Brazil) in a decommissioning operation. Environ Earth Sci 62:857–863

Canovas CR, Olias M, Nieto JM, Sarmiento AM, Ceron JC (2007) Hydrogeochemical characteristics of the Tinto and Odiel Rivers (SW Spain). Factors controlling metal contents. Sci Total Environ 373:363–382

Chadha DK (1999) A proposed new diagram for geochemical classification of natural waters and interpretation of chemical data. Hydrogeol J 7:431–439

Cipriani M (2002) Mitigation of social and environmental impacts caused by the definitive closure of uranium mines, Ph.D. Thesis (in Portuguese), State University of Campinas

Custódio E (1983) Princípios básicos de química y radioquímica de aguas subterrâneas. In: Custódio E, Llamas MR (ed) Hidrologia Subterrânea. Barcelona: Ediciones Omega. 2. Ed., Tomo 1, Sección 4, pp 174–246

Drever JI (1997) The geochemistry of natural waters, surface and groundwater environments, 3rd edn. Prentice Hall, New Jersey

Fernandes HM, Franklin MR (2001) Assessment of acid rock drainage pollutants released at the uranium mining site of Poços de Caldas—Brazil. J Environ Radioact 54:5–25

Fernandes HM, Veiga LHS, Franklin MR, Prado VCS, Taddei JF (1995) Environmental impact assessment of uranium and milling facilities: a study case at the Poços de Caldas uranium mining and milling site, Brazil. J Geochem Explor 52:161–173

Fernandes HM, Franklin MR, Veiga LHS, Freitas P, Gomiero LA (1996) Management of uranium mill tailing: geochemical process and radiological risk assessment. J Environ Radioact 30:69–95

Fernandes HM, Franklin MR, Veiga LHS (1998) Acid rock drainage and radiological environmental impacts: a study case of the Uranium mining and milling facilities at Poços de Caldas. Waste Manag 18:169–181

Fernandes HM, Franklin MR, Gomiero MR (2008) Critical analysis of the waste management performance of two uranium production units in Brazil-part I: Poços de Caldas production centre. J Environ Manage 87:59–72

Fetter CW (1994) Applied hydrogeology, 4th edn. Prentice Hall, New Jersey

Franklin MR (2007) Numerical modeling of water flow and geochemical processes applied to the prediction of acid drainage at a waste rock pile in the uranium mine of Poços de Caldas—MG, Ph.D. Thesis, Federal University of Rio de Janeiro

Garrals RM, Christ CL (1965) Solutions, minerals, and equilibria. Harper and Row, New York

Golder Associates Brazil Consulting and Projects Ltd. (2012) Plan for de Recovery of Degraded areas—INB UTM Caldas. Technical Report No. RT-006_099-515-3023_01-j

Gomes AFS, Lopez DL, Ladeira ACQ (2012) Characterization and assessment of chemical modifications of metal-bearing sludges arising from unsuitable disposal. J Hazard Mater 199–200: 418–425

Jambor JL (2003) Mine-waste mineralogy and mineralogical perspectives of acid-basic accounting. In: Jambor JL, Blowes DW, Ritchie AIM (eds) Environmental aspects of mine wastes. Mineralogical Association of Canada, Vancouver, pp 117–145

Majdalani AA, Tavares AM (2001) Status of uranium in Brazil. In: Assessment of uranium deposit types and resources — a worldwide perspective. In: Proceedings of a Technical Committee Meeting organized by the International Atomic Energy Agency and the OECD Nuclear Energy Agency and held in Vienna, IAEA TECDOC 1258, December 2001. International Atomic Energy Agency, Viena

Ptacek CJ, Blowes DW (2003) Geochemistry of concentrated waters at mine-waste sites. In: Jambor JL, Blowes DW, Ritchie AIM (eds) Environmental aspects of mine wastes. Mineralogical Association of Canada, Vancouver, pp 239–251

Rodgher S, Azevedo H, Ferrari CR, Roque CV, Ronqui LB, Campos MB, Nascimento MRL (2013) Evaluation of surface water

quality in aquatic bodies under the influence of uranium mining (MG, Brazil). Environ Monit Assess 185:2395–2406

Schorscher HD, Shea ME (1992) The regional geology of the Poços de Caldas alkaline complex: mineralogy and geochemistry of selected nepheline syenites and phonolites. J Geochem Explor 45:25–51

U. S. EnvironmentaL Protection Agency—USEPA (1994) Acid mine drainage prediction. Office of Solid Waste, Washington DC

Waber N, Schorscher HD, Peters T (1992) Hydrothermal and supergene uranium mineralization at the Osamu Utsumi mine, Poços de Caldas, Minas Gerais, Brazil. J Geochem Explor 45:53–112

Williams RE (1975) Waste production and disposal in mining, milling, and metallurgical industries. Miller-Freeman Publishing Company, San Francisco

Williamson MA, Rimstidt JD (1994) The kinetics and electrochemical rate-determining step of aqueous pyrite oxidation. Geochim Cosmochim Acta 58:5443–5454

Wooley AR (1987) Alkaline rocks and carhonatites of the World, Part 1. North and South America. British Museum (Natural History), London, p 216